J. Fluid Mech. (2003), *vol.* 497, *pp.* 1–22. © 2003 Cambridge University Press
DOI: 10.1017/S0022112003006426 Printed in the United Kingdom

Effects of small-amplitude fluctuations on the structure of a shock wave

By P. L. RENDÓN AND D. G. CRIGHTON†

Department of Applied Mathematics and Theoretical Physics, University of Cambridge, Centre for Mathematical Sciences, Wilberforce Road, Cambridge CB3 0WA, UK

(Received 27 September 2000 and in revised form 25 July 2003)

A thermoviscous steady shock is studied through its interaction with small-amplitude perturbations introduced far behind the shock region and convected uniformly towards it. It is assumed that a significant broadening of the shock region may be brought about by the amplification of the fluctuations as they pass through it. The scale of such broadening effects, however, is found to depend on the amplitude and frequency of the induced fluctuations. Indeed, well-defined ranges of these parameters determine the scale of the non-uniform part of the mean flow, and thus, of any effects observed inside the shock region. For specific values of these parameters, we observe not only a broadening, but also a deformation of the shock region. These results are confirmed numerically using a pseudospectral scheme.

1. Introduction

In this paper we are concerned with the study of the structure of a thermoviscous steady shock as it interacts, after some time, with small-amplitude fluctuations introduced far behind the shock region. When dealing with nonlinear waves travelling in non-dispersive media, the plane Burgers equation is often used as the simplest model equation which exhibits both a nonlinear redistribution of energy across the spectrum and the diffusive effects of viscosity over a small region; here, it is given as

$$u_t + uu_x = \nu u_{xx}. \tag{1.1}$$

It is interesting to point out that for $\nu = 0$ the plane Burgers equation (1.1) becomes quite simply a scalar hyperbolic equation. For this type of equation, shocks appear only as sharp discontinuities, and it was precisely because of this shortcoming that equation (1.1) was suggested as a model capable of describing the structure of shock waves in gas dynamics. From the study of the exact solutions to the ordinary Burgers equation, we know that shocks will form in any wave with a compressive phase. For moderate ranges we can use 'weak-shock theory' to predict the location of these shocks and to determine their interior structure, which is resolved by thermoviscous attenuation and is described by Taylor's hyperbolic tangent solution. Taylor (1910) obtained the thickness of the transitional region that results when rapid changes in pressure are mitigated by diffusive effects, but he did not, however, establish the relationship between shocks of this form and the Burgers equation. This task was achieved later, by for example Bateman (1915) and Burgers (1948) himself.

† David Crighton died in April 2000 during the preparation of this paper.

In the present work we study the low-diffusivity limit of the plane Burgers equation when small-amplitude fluctuations are introduced behind the shock region. One of the principal motivations behind this work concerns with observations on the manner in which the generation of fluctuations influences the spatial width of shocks, also known as shock rise time. This topic is discussed, for hydraulic jumps, by Martín Vide, Dolz & del Estal (1993), for a shock induced in a thermoviscous fluid by the action of an impulsive piston, by Moran & Shen (1993), and in more general circumstances, by Dowling & Ffowcs Williams (1983), and Ffowcs Williams (1992). Averaging of the mean profiles over a time cycle determined by the fluctuations yields a broadening and a particular deformation of the shock profile, but only for very specific values of the amplitude and frequency of the induced fluctuations. Thus, we have used two parameters to determine a family of solutions such that the above behaviour is observed. To obtain these results we have proceeded in the usual manner, first using asymptotic analysis to obtain approximate solutions to the problem at hand, and then implementing numerical methods, in this case a pseudospectral scheme, to confirm the validity of these solutions.

2. Shock wave distortion due to fluctuations behind the shock

2.1. *A simple model*

In order to justify the approach which we employ in § 2.2, which contains the main results of this paper, we discuss here a simple model where we consider a single fluctuation introduced far behind a steady shock, and which is initially rigidly convected, moving in the direction of the x-axis. We seek some deformation of a region behind the shock caused by the introduction of this fluctuation. We thus begin by considering the plane Burgers equation

$$u_t + uu_x = \nu u_{xx}, \tag{2.1}$$

where the velocity $u(x,t)$ is prescribed everywhere at a time t_0; t is time, x is a spatial coordinate in the frame of reference moving with the small-signal sound speed a_0, and ν is the diffusivity term. We are interested in solutions of the form $u(x,t) = U(x)+u'(x,t)$, where $u'(x,t)$ is a fluctuation amplitude and $U(x)$ is the mean field that results from time-averaging over a random field of fluctuations behind a steady shock wave, measured with respect to axes in which the mean profile $U(x)$ is at rest. By choosing the mean profile to be at rest in terms of the x-coordinate we are, in fact, requiring the following boundary condition:

$$\lim_{x\to-\infty} U(x) + \lim_{x\to\infty} U(x) = 0. \tag{2.2}$$

Substituting the desired form of the solution in equation (2.1), and averaging this equation over time, where we use $\langle\,\rangle$ to denote this operation, we arrive at the exact mean and fluctuation equations:

$$UU_x + \langle u'u'_x\rangle = \nu U_{xx}, \tag{2.3}$$

$$u'_t + Uu'_x + u'U_x + u'u'_x - \langle u'u'_x\rangle = \nu u'_{xx}. \tag{2.4}$$

Above, we have also used the fact that $\langle u'\rangle = 0$. Now we continue by effectively expanding both equations in powers of a small dimensionless amplitude u'/U, to obtain

$$U_0U_{0_x} = \nu U_{0_{xx}}, \tag{2.5}$$

$$u'_t + U_0u'_x + u'U_{0_x} = \nu u'_{xx}. \tag{2.6}$$

The solution to (2.5) is given by

$$U_0(x) = -U_+ \tanh \frac{U_+ x}{2\nu}, \qquad \text{where } \lim_{x\to\pm\infty} U_0(x) = \mp U_+, \tag{2.7}$$

which is the Taylor description of a thermoviscous steady shock in the absence of fluctuations, and which exhibits the same behaviour as the mean profile $U(x)$ when $x \to -\infty$, as given by the boundary condition (2.2); this solution is discussed in detail by, among others, Whitham (1974). It is clear that further terms in this expansion must be obtained so as to observe the behaviour sought, but first we will analyse the propagation of the fluctuation behind the shock. In the following analysis, then, we will be concerned only with the region behind the shock, $x < 0$. For the solution of equation (2.6) it is necessary to consider an inner solution in the vicinity of the shock to smooth out the discontinuity of an outer, lossless solution in this region (Van Dyke 1975). Now assume that as $x \to -\infty$ the field $u'(x, t)$ has a typical magnitude u_0 (for example, the root mean square of the velocity perturbation), and a length scale L. For x large and negative, we know the fluctuations to be rigidly convected,

$$u'_t + U_+ u'_x = 0; \tag{2.8}$$

and from this expression we conclude that the time scale to use as $x \to -\infty$ is L/U_+. We can now consider equation (2.6) with $U_0(x)$ given by the Taylor shock solution (2.7), and with the appropriate dimensionless variables $\hat{u} = u'/u_0$, $\hat{x} = x/L$, $\hat{t} = U_+ t/L$:

$$\frac{U_+ u_0}{L}\hat{u}_{\hat{t}} - \frac{U_+ u_0}{L}\tanh\left(\frac{U_+ L\hat{x}}{2\nu}\right)\hat{u}_{\hat{x}} - u_0\,\hat{u}\,\frac{U_+^2}{2\nu}\operatorname{sech}^2\left(\frac{U_+ L\hat{x}}{2\nu}\right) = \frac{\nu u_0}{L^2}\hat{u}_{\hat{x}\hat{x}}.$$

Writing $R = U_+ L/\nu \gg 1$, with R a Reynolds number, relating the contribution of nonlinearity to that of diffusivity, dropping the hats, and simplifying the above expression, we obtain

$$u_t - \tanh\left(\tfrac{1}{2}Rx\right)u_x - \tfrac{1}{2}Ru\operatorname{sech}^2\left(\tfrac{1}{2}Rx\right) = \frac{1}{R}\,u_{xx}. \tag{2.9}$$

For $(x, t) = O(1)$, and since $R \gg 1$, we have

$$u_t - u_x = 0, \tag{2.10}$$

which gives us the outer solution

$$u_{out}(x, t) = v(t + x), \tag{2.11}$$

where, as $x \to -\infty$, $u' \sim u_0 v(t + x)$. This lossless solution is clearly invalid when the inner variable $X = Rx = O(1)$. In this region we rewrite equation (2.9) in terms of $\zeta = \frac{1}{2}X$ and a small parameter $\delta = 2/R$ as

$$\delta\frac{\partial u}{\partial t} - \frac{\partial}{\partial\zeta}(u\tanh\zeta) = \frac{1}{2}\frac{\partial^2 u}{\partial\zeta^2}. \tag{2.12}$$

To leading order, this equation yields the general inner solution to the problem, given by

$$u_{in}(\zeta, t) = C_1(t)\operatorname{sech}^2\zeta + C_2(t)(\zeta\operatorname{sech}^2\zeta + \tanh\zeta). \tag{2.13}$$

Notice that ζ has been defined so as to be a Taylor variable, the natural coordinate of the Taylor shock solution, so that $U_0 = U_+ \tanh\zeta$. It is now possible to match the

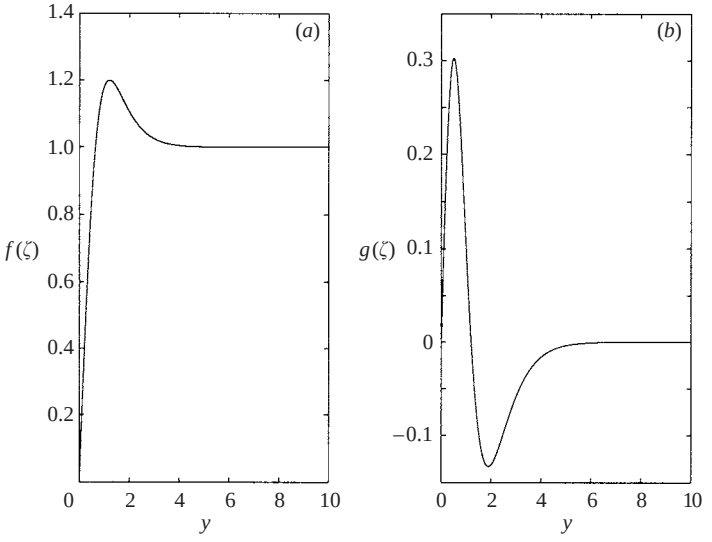

FIGURE 1. (*a*) The function $f(\zeta)$ defined by (2.16); (*b*) the function $g(\zeta)$ defined by (2.23).

inner and outer solutions, for $x < 0$, by equating

$$\lim_{\zeta\to\infty} u_{in} = \lim_{x\to 0^-} u_{out},$$

so as to obtain $C_2(t) = v(t)$.

To obtain $C_1(t)$ we require the $O(\delta)$ part of equation (2.12) to vanish as well, giving as a result

$$\left.\frac{\partial u_{in}}{\partial t}\right|_{\zeta=0} = 0. \tag{2.14}$$

From (2.13) we have that $u_{in}(\zeta = 0, t) = C_1(t)$, and thus, we see that $C_1(t) = \text{constant} = C$. In this case, though, $C\,\text{sech}^2\zeta$ is a steady quantity, and corresponds simply to a change in the origin of the mean profile, so that if we take C to be already accounted for in the choice of origin, we can then simply choose $C = 0$, in which case the inner solution is given by

$$u_{in} = v(t) f(\zeta), \tag{2.15}$$

$$f(\zeta) = \zeta\,\text{sech}^2\zeta + \tanh\zeta. \tag{2.16}$$

The multiplicative composite solution, formed from (2.11) and (2.15) will then be

$$u(x, t) \sim v(t - x) f(\zeta). \tag{2.17}$$

A simple analysis of $f(\zeta)$, given by (2.16), reveals that as $\zeta \to \infty$, $f(\zeta) \to 1$, and since $\tanh\zeta \sim \zeta$ for very small ζ, $f(\zeta) \sim 2\zeta$ for $\zeta \to 0^+$. After calculating $f'(\zeta)$ and equating to zero, we see that a maximum will occur for $\tanh\zeta_M = \zeta_M$; this maximum value is $f_M = f(\zeta_M) = \zeta_M(1 - \zeta_M^{-2}) + \zeta_M^{-1} = \zeta_M$. The function $f(\zeta)$ is illustrated in figure 1(*a*). The fluctuation amplitude is seen to remain almost constant outside the inner region, but as the fluctuation enters this region, the amplitude first increases, and then rapidly decreases.

If we now return to dimensional variables and expand the mean field again in terms of a small, dimensionless parameter, now u_0/U_+, as $U = U_0 + (u_0/U_+)^2 U_2 + \cdots$, the

full equation for the mean field (2.3) becomes

$$\left(\frac{u_0}{U_+}\right)^2 \frac{\partial}{\partial x}(U_0U_2) + U_0\frac{\partial U_0}{\partial x} + \left(\frac{u_0}{U_+}\right)^4 U_2\frac{\partial U_2}{\partial x} + \left(\frac{u_0}{U_+}\right)^2 \frac{U_+^2}{2}\frac{\partial}{\partial x}\langle u^2\rangle = \nu\left(\frac{\partial^2 U_0}{\partial x^2} + \left(\frac{u_0}{U_+}\right)^2 \frac{\partial^2 U_2}{\partial x^2}\right),$$

and, since $u' = O(u_0)$, we match second-order terms to obtain

$$\frac{\partial}{\partial x}(U_0U_2) + \frac{U_+^2}{2}\frac{\partial}{\partial x}\langle u^2\rangle = \nu\frac{\partial^2 U_2}{\partial x^2}. \tag{2.18}$$

If we consider, as before, that away from the shock region the diffusive term may be neglected, and consider as well that $U_2 \to 0$ as $x \to -\infty$, this equation can be integrated, from $x \to -\infty$ to $x < 0$, to give

$$U_0U_2 + \frac{U_+^2}{2}\langle u^2\rangle = \frac{U_+^2}{2}, \tag{2.19}$$

which is an algebraic equation that can be solved easily using the fact that $\langle v^2\rangle = 1$, and thus $\langle u^2\rangle = f^2(\zeta)$:

$$U_2 = \frac{U_+(1 - f^2(\zeta))}{2\tanh\zeta}. \tag{2.20}$$

The mean flow correction U_2, though, becomes very large for $\zeta \to 0^-$, which indicates that the effects of diffusion cannot be neglected in the vicinity of the shock, and thus, in this inner region, the diffusive term should be reinstated. This time, by integrating from $-\infty$ to x, we obtain, instead of an algebraic equation for U_2 as in (2.19), a differential equation,

$$U_0U_2 + \frac{U_+^2}{2}(\langle u^2\rangle - 1) = \nu\frac{\partial U_2}{\partial x}. \tag{2.21}$$

Integrating once more we arrive at

$$U_2 = -D\left(\frac{U_+}{u_0}\right)^2 \operatorname{sech}^2\zeta + U_+(\zeta\operatorname{sech}^2\zeta - \zeta^2\tanh\zeta\operatorname{sech}^2\zeta),$$

where D is a constant which, as was the case with C, can be absorbed into the definition of U_0. This solution can be written, alternatively, as

$$U_2(x) = U_+ g(\zeta), \tag{2.22}$$

$$g(\zeta) = \zeta\operatorname{sech}^2\zeta(1 - \zeta\tanh\zeta), \tag{2.23}$$

where $g(\zeta)$ can be analysed in much the same way $f(\zeta)$ was. To first order, $g(\zeta) \sim \zeta$ as $\zeta \to 0$, and $\zeta \to 0^-$ as $\zeta \to \infty$, so this function has at least one zero for $\zeta > 0$. Equating the derivative of $g(\zeta)$ to zero to look for critical points, we obtain the condition $1 - 4\zeta\tanh\zeta - \zeta^2(1 - 3\tanh^2\zeta) = 0$; two roots exist for $\zeta > 0$, and they are approximately $\zeta_1 = 5^{-1/2}$ and $\zeta_2 = 1 + 2^{-1/2}$, the first one corresponding to a maximum and the second to a minimum; see figure 1(*b*). It is not difficult to see that these results can be carried through $\zeta = 0$, and that the fields u', U_2 decay monotonically and exponentially ahead of the shock.

The unsophisticated model employed in this section has permitted the observation of an interesting effect: a region behind the shock is seen where the fluctuations cause

the gradient $\partial U/\partial x$ to be affected, albeit to a small degree, by the Reynolds stress $\langle u'^2\rangle$. Elsewhere, the gradient is controlled by the viscous stress, as it would be in the absence of fluctuations. We would like to observe, however, such an effect to take place at a larger scale; the effects of these fluctuations are very small, uniformly $O(u_0^2/U_+^2)$ relative to the undisturbed components. Experiments on hydraulic jump propagation suggest that more noticeable effects should be produced by these fluctuations. The fluctuations in this case fail to produce larger-scale effects because they are uniformly convected (see (2.17)) everywhere except for a narrow region of width $x = O(1/R)$, where they are quickly suppressed by diffusion. In order to observe a more significant amplification of the fluctuations in the mean flow we must broaden the scale of the non-uniform part of the mean flow to values much larger than $1/R$, and this broadening must be itself due to the fluctuations as they amplify. In the next section we construct a self-consistent model in which the field in which the fluctuations propagate is determined mainly by the fluctuations themselves.

2.2. *A self-consistent mean field theory*

In the previous section, we assumed the mean profile was given by the Taylor hyperbolic tangent solution corrected by a small perturbation which only became significant in a thin region behind the shock centre. In the following analysis, the only assumptions made with regard to the mean profile concern its behaviour close to the origin and as x tends to infinity in both directions. Crucially, the Reynolds stress term in the mean field equation (2.3) is retained, and will eventually determine the conditions necessary for a significant broadening of the shock region and distortion of the shock profile to occur. We again start from the mean and fluctuation equations (2.3) and (2.4), and again we linearize (2.4) in u':

$$u'_t + Uu'_x + u'U_x = \nu u'_{xx}. \tag{2.24}$$

We now also integrate (2.3):

$$\frac{1}{2}\frac{\mathrm{d}U^2}{\mathrm{d}x} + \frac{1}{2}\frac{\partial\langle u'^2\rangle}{\partial x} = \nu\frac{\mathrm{d}U_x}{\mathrm{d}x},$$

supposing that far behind the shock $U \to U_-$ and the Reynolds stress $\langle u'^2\rangle \to u_0^2$, and far ahead of the shock $U \to -U_+$, $\langle u'^2\rangle \to 0$, with both U_+, U_- strictly positive. Integrating once more, now from $-\infty$ to x, we obtain the mean field equation,

$$\tfrac{1}{2}U^2 + \tfrac{1}{2}\langle u'^2\rangle = \nu U_x + \tfrac{1}{2}U_+^2, \tag{2.25}$$

and integrating now from $-\infty$ to $+\infty$ we see that

$$U_-^2 + u_0^2 = U_+^2. \tag{2.26}$$

There are two independent dimensionless parameters that we will consider for this problem: the first is a fluctuation amplitude $\epsilon = u_0/U_-$, and the second is a Reynolds number $R_- = U_-^2/2\nu\omega$, where ω is a typical frequency of the fluctuations. We take the origin of coordinates to be such that $U(0) = 0$, and assume

$$U \sim -\beta x \quad \text{near } x = 0, \tag{2.27}$$

for some $\beta > 0$ which will be determined later from a nonlinear eigenvalue problem. We now transform $u'(x, t)$ as follows:

$$u'(x, t) = \int_{-\infty}^{\infty} \tilde{u}(x, \omega)\, \mathrm{e}^{-\mathrm{i}\omega t}\, \mathrm{d}\omega, \tag{2.28}$$

so that (2.24) becomes

$$U\tilde{u}_x + (U_x - \mathrm{i}\omega)\tilde{u} = \nu\tilde{u}_{xx}. \tag{2.29}$$

We can easily find a solution to the above equation if we ignore the diffusive term, by using the integrating factor $\exp(-\mathrm{i}\omega\Phi(x))$, where

$$\Phi(x) = \frac{x}{U_-} + \int_{-\infty}^{x} \left(\frac{1}{U(s)} - \frac{1}{U_-} \right) \mathrm{d}s.$$

The use of this integrating factor permits us to write equation (2.29) as follows:

$$\frac{\mathrm{d}}{\mathrm{d}x} \left[U(x)\mathrm{e}^{-\mathrm{i}\omega\Phi(x)}\tilde{u}(x,\omega) \right] = 0,$$

and thus

$$\tilde{u}(x,\omega) = \frac{f(\omega)}{U(x)}\mathrm{e}^{\mathrm{i}\omega\Phi(x)}, \tag{2.30}$$

with $f(\omega)$ still to be determined. We now consider $\tilde{v}(\omega)$ to be the Fourier component of $u'(x,t)$ as $x \to -\infty$ such that

$$\begin{aligned} \lim_{x\to-\infty} u'(x,t) &= v'\left(t - \frac{x}{U-} \right) \\ &= \int_{-\infty}^{\infty} \tilde{v}(\omega)\mathrm{e}^{-\mathrm{i}\omega(t-x/U_-)}\,\mathrm{d}\omega, \end{aligned}$$

which simply means that fluctuations will be rigidly convected at speed U_- for x very large and negative, up to a point where $u'(x,t)$ deviates from U_- and its evolution is characterized by the amplification and distortion factors seen in equation (2.30), which we write in the following manner:

$$\tilde{u}(x,\omega) = \frac{U_-}{U(x)}\tilde{v}(\omega)\mathrm{e}^{\mathrm{i}\omega\Phi(x)}. \tag{2.31}$$

It will now be possible to obtain the Reynolds stress $\langle u'^2(x,t)\rangle$ when $x \to -\infty$, since, from (2.31) and the definition of $\tilde{v}(\omega)$,

$$\begin{aligned} u'(x,t) &= \frac{U_-}{U(x)} \int_{-\infty}^{\infty} \tilde{v}(\omega)\mathrm{e}^{-\mathrm{i}\omega(t-\Phi(x))}\,\mathrm{d}\omega \\ &= \frac{U_-}{U(x)} v'(t - \Phi(x)), \end{aligned}$$

and then

$$\langle u'^2(x,t)\rangle = \left(\frac{U_-}{U(x)} \right)^2 u_0^2,$$

where $\langle u'^2(x,t)\rangle \to \langle v'^2(t)\rangle = u_0^2$ as $x \to -\infty$.

However, we can easily see that the solution (2.31) is not uniformly valid near $x = 0$ by analysing the orders of magnitude of each of the four terms in equation (2.29) in this region, using both (2.27) and (2.31) for this purpose:

$$\begin{aligned} U\tilde{u}_x &= O(U_-/x), \\ U_x\tilde{u} &= O(U_-/x), \\ \mathrm{i}\omega\tilde{u} &= O(\omega U/\beta x), \\ \nu\tilde{u}_{xx} &= O(\nu U_-/\beta x^3). \end{aligned}$$

It will be clear now that we cannot readily ignore the diffusive term in the region near $x=0$, and thus for this inner region we employ a self-consistent approach, in which we must consider all four terms as comparable, with no assumptions regarding the order of β made until its defining equation is found. The one simplification we will make consists of considering $U \sim -\beta x$, as in (2.27), so that $\mathrm{d}U/\mathrm{d}x \sim -\beta$, and then substituting in equation (2.29), so that in some inner region we have

$$-\beta x \tilde{u}_x - (\beta + \mathrm{i}\omega)\tilde{u} = \nu \tilde{u}_{xx}, \tag{2.32}$$

which we will transform using the following change of variables:

$$x = \sqrt{\frac{\nu}{\beta}}\xi, \qquad \tilde{u}(x,\omega) = \mathrm{e}^{-\beta x^2/4\nu}\Psi(\xi,\omega), \tag{2.33}$$

so that

$$\tilde{u}_x = \mathrm{e}^{-\beta x^2/4\nu}\left(-\frac{\beta x}{2\nu}\Psi + \sqrt{\frac{\beta}{\nu}}\Psi_\xi\right),$$

$$\tilde{u}_{xx} = \mathrm{e}^{-\beta x^2/4\nu}\left\{\left[\left(\frac{\beta x}{2\nu}\right)^2 - \frac{\beta}{2\nu}\right]\Psi - x\left(\frac{\beta}{\nu}\right)^{3/2}\Psi_\xi + \frac{\beta}{\nu}\Psi_{\xi\xi}\right\}.$$

The resulting equation will be Weber's equation,

$$\Psi_{\xi\xi} + \left(\frac{1}{2} + \frac{\mathrm{i}\omega}{\beta} - \frac{\xi^2}{4}\right)\Psi = 0, \tag{2.34}$$

the solutions of which are the parabolic cylinder functions, D in the notation of Whittaker & Watson (1980). If we now introduce a Strouhal number $\sigma = \omega/\beta$, which relates the frequency to the inverse of the time in which a given particle crosses the inner region, we can write the general solution to the problem as a sum of two linearly independent solutions,

$$\Psi(\xi,\omega) = A(\omega)D_{\mathrm{i}\sigma}(\xi) + B(\omega)D_{-\mathrm{i}\sigma-1}(\mathrm{i}\xi), \tag{2.35}$$

which is an analytical expression, and thus removes the singularity present in the outer solution at $x=0$. We will now use asymptotic matching to determine A and B in order to obtain the necessary transition expression through $x=0$; it will be necessary to use asymptotic expansions of the parabolic cylinder functions for large $|\xi|$. From Whittaker & Watson we know that for large ξ and $|\arg\xi| < \frac{3}{4}\pi$,

$$D_n(\xi) \sim \mathrm{e}^{-\xi^2/4}\xi^n\left[1 - \frac{n(n-1)}{2\xi^2} + \frac{n(n-1)(n-2)(n-3)}{2\times 4\xi^4} - \cdots\right], \tag{2.36}$$

so that, in our case, using only the first term of the above expansion, for $\xi \to \infty$,

$$\Psi \sim \left[A\mathrm{e}^{-\xi^2/4}\xi^{\mathrm{i}\sigma} + B\mathrm{e}^{\xi^2/4}\left(\mathrm{e}^{\mathrm{i}\pi/2}\xi\right)^{-\mathrm{i}\sigma-1}\right](1 + O(\xi^{-2})). \tag{2.37}$$

If we were to set $B=0$, the above field would decay very rapidly ahead of the shock; in fact, it would do so like $\exp(-\xi^2/2)$. If, on the other hand, we were to set $A=0$, the field would decay like ξ^{-1} ahead of the shock, which is to say very slowly indeed; in this case it would not be possible to match this solution to the outer solution given by (2.31). Thus, we set $B=0$ and now proceed to determine the value of A by matching these solutions. The appropriate expansion as $\xi \to -\infty$, with $B=0$, is given

by

$$\Psi \sim A\frac{\sqrt{2\pi}}{\Gamma(-\mathrm{i}\sigma)}\mathrm{e}^{-\pi\sigma+\xi^2/4}(\mathrm{e}^{\mathrm{i}\pi}|\xi|)^{-\mathrm{i}\sigma-1}, \tag{2.38}$$

and reverting to the original variables by means of (2.33) this expression becomes

$$\tilde{u}(x,\omega) \sim A\frac{\sqrt{2\pi}}{\Gamma(-\mathrm{i}\sigma)}\left(\frac{\beta}{\nu}|x|\right)^{-\mathrm{i}\sigma-1}. \tag{2.39}$$

This solution must now be made to match the inner asymptotics of (2.31), and in doing so we will find the appropriate value of $A(\omega)$. The solution (2.31) as $x \to 0^-$ is given by

$$\tilde{u}(x,\omega) \sim \frac{U_-|x|^{\mathrm{i}\sigma}}{\beta|x|}\tilde{v}(\omega)\mathrm{e}^{\mathrm{i}\omega\Omega}, \tag{2.40}$$

where

$$\Omega(x) = \frac{\ln|x_0|}{\beta} + \int_{-\infty}^{x_0}\left(\frac{1}{U(s)} - \frac{1}{U_-}\right)\mathrm{d}s + \int_{x_0}^{0}\left(\frac{1}{U(x)} - \frac{1}{(-\beta s)} - \frac{1}{U_-}\right)\mathrm{d}s,$$

for an arbitrary $x_0 < 0$.

It now becomes straightforward to match inner and outer solutions as $x \to 0^-$; by doing so, we obtain the previously undetermined value of A:

$$A(\omega) = \frac{\Gamma(-\mathrm{i}\sigma)}{\sqrt{2\pi}}\left(\frac{\beta}{\nu}\right)^{(\mathrm{i}\sigma+1)/2}\frac{U_-\tilde{v}(\omega)}{\beta}\mathrm{e}^{\mathrm{i}\Omega}. \tag{2.41}$$

Since $\Psi = A(\omega)D_{\mathrm{i}\sigma}(\xi)$, we now have, by virtue of (2.33),

$$\tilde{u}(x,\omega) = \mathrm{e}^{-\beta x^2/4\nu}A(\omega)D_{\mathrm{i}\sigma}(\xi),$$

and since we will, in the end, be interested in calculating the Reynolds stress, or fluctuation energy, $\langle u'^2(x,t)\rangle$, we combine this inner solution and the outer solution (2.31) in a multiplicative composite,

$$\begin{aligned}\tilde{u}(x,\omega) &\sim \frac{\left[\dfrac{U_-}{U(x)}\tilde{v}(\omega)\mathrm{e}^{\mathrm{i}\omega\Phi(\omega)}\right]\left[\mathrm{e}^{-\beta x^2/4\nu}A(\omega)D_{\mathrm{i}\sigma}(\xi)\right]}{\dfrac{\sqrt{2\pi}}{\Gamma(-\mathrm{i}\sigma)}A(\omega)\left(\dfrac{\nu}{\beta}\right)^{(\mathrm{i}\sigma+1)/2}|x|^{-\mathrm{i}\sigma-1}} \\ &= \frac{\Gamma(-\mathrm{i}\sigma)}{\sqrt{2\pi}}\left(\frac{\beta}{\nu}\right)^{(\mathrm{i}\sigma+1)/2}\frac{U_-|x|}{U(x)}D_{\mathrm{i}\sigma}(\xi)\tilde{v}(\omega)\exp\left(-\frac{\beta x^2}{4\nu} + \mathrm{i}(\omega\Phi + \sigma\ln|x|)\right),\end{aligned} \tag{2.42}$$

which is clearly finite at $x = 0$ since $U(x) \sim -\beta x$ in the vicinity of this point.

For $x > 0$ we want the fluctuations to decay very rapidly ahead of the shock, so we simply use the inner solution

$$u(x,\omega) = A\mathrm{e}^{-\beta x^2/4\nu}$$

for the entire domain. Referring to (2.37), we can establish that this solution will decay like $\exp(-\beta x^2/2\nu)$ ahead of the shock.

2.3. *Spectral representation*

The power spectral density of a given function is the Fourier transform of its autocorrelation function, and it essentially represents the average rate of energy flow.

Using the Fourier inversion theorem we may express the fluctuation energy $\langle u'^2(x,t)\rangle$ in terms of its power spectral density $S(x,\omega)$,

$$\langle u'^2(x,t)\rangle = \int_{-\infty}^{\infty} S(x,\omega)\,\mathrm{d}\omega, \tag{2.43}$$

so that

$$\langle \tilde{u}(x,\omega)\tilde{u}(x,\omega')\rangle = S(x,\omega)\delta(\omega+\omega'). \tag{2.44}$$

For more information on the statistical properties and manipulation of spectra and their Fourier transforms, we refer the reader to books by Gurbatov, Malakhov & Saichev (1991) and Lumley (1970). Using the multiplicative composite (2.42) in this last expression, we arrive at

$$\begin{aligned} S(x,\omega)\delta(\omega+\omega') = {} & \frac{\Gamma(-\mathrm{i}\sigma)\Gamma(-\mathrm{i}\sigma')}{2\pi}\left(\frac{U_-|x|}{U(x)}\right)^2\left(\frac{\beta}{\nu}\right)^{\mathrm{i}(\sigma+\sigma')/2} D_{\mathrm{i}\sigma}(\xi)D_{\mathrm{i}\sigma'}(\xi) \\ & \times \langle \tilde{v}(\omega)\tilde{v}(\omega')\rangle \exp\left(-\tfrac{1}{2}\xi^2 + \mathrm{i}(\omega+\omega')\left(\Phi + \frac{1}{\beta}\ln|x|\right)\right), \end{aligned} \tag{2.45}$$

where σ' corresponds to ω'. At this point we introduce $S_0(\omega)$, the power spectral density of the convected fluctuations as $x\to-\infty$, such that $\langle \tilde{v}(\omega)\tilde{v}(\omega')\rangle = S_0(\omega)\delta(\omega+\omega')$. Therefore,

$$\begin{aligned} \frac{S(x,\omega)}{S_0(\omega)} &= \frac{|\Gamma(-\mathrm{i}\sigma)|^2}{2\pi}\left(\frac{U_-|x|}{U(x)}\right)^2\frac{\beta}{\nu}|D_{\mathrm{i}\sigma}(\xi)|^2\mathrm{e}^{-\xi^2/2} \\ &= \frac{1}{2\nu\omega\sinh\pi\sigma}\left(\frac{U_-\beta|x|}{U(x)}\right)^2|D_{\mathrm{i}\sigma}(\xi)|^2\mathrm{e}^{-\xi^2/2}, \end{aligned} \tag{2.46}$$

where we have used the relation $|\Gamma(-\mathrm{i}\sigma)|^2 = \pi/(\sigma\sinh\pi\sigma)$. This equation is a basic result of this theory, giving the power amplification of any given spectral component in an arbitrary mean field $U(x)$ such that (2.27) is valid near $x=0$.

Let us now consider only narrowband fluctuations of the form

$$S_0(\omega) = \tfrac{1}{2}u_0^2[\delta(\omega-\omega_0)+\delta(\omega+\omega_0)], \tag{2.47}$$

so that the fluctuation energy is concentrated within a frequency band of width $2\omega_0$. This bandwidth is determined by the autocorrelation of the signal $v'(t)$, which is of the form $\cos(\omega_0 t)$; notice that $S_0(\omega)$ is essentially the Fourier transform of such a cosine wave. Integration of equation (2.46) is straightforward after we have substituted this form of $S_0(\omega)$ in the equation; we obtain

$$\langle u'^2(x,t)\rangle = \frac{u_0^2}{2\nu\omega\sinh\pi\sigma}\left(\frac{U_-\beta|x|}{U(x)}\right)^2|D_{\mathrm{i}\sigma}(\xi)|^2\mathrm{e}^{-\xi^2/2}, \tag{2.48}$$

where we have dropped the suffix 0 from ω, and consequently from σ as well. Notice that ω and u_0, the frequency and amplitude of the fluctuations introduced behind the shock, completely determine the values of the two parameters introduced previously, R_- and ϵ, since $U_\pm$ and ν are fixed. They will be seen to determine families of solutions for which the process of averaging over time will yield very different results with respect to the mean profile. The regions to which these different results correspond will be established in the next section.

2.4. *A nonlinear eigenvalue problem*

The mean field equation (2.25) can be used to set up an eigenvalue problem which we can use to determine the values of β that correspond to different values of the parameters discussed in the previous section. We begin by substituting the expression for the fluctuation energy (2.48) into the mean field equation (2.25):

$$\tfrac{1}{2}U^2(x) + \frac{u_0^2}{4\nu\omega\sinh\pi\sigma}\left(\frac{U_-\beta|x|}{U(x)}\right)^2 |D_{\mathrm{i}\sigma}(\xi)|^2 \mathrm{e}^{-\xi^2/2} = \nu\frac{\mathrm{d}U}{\mathrm{d}x} + \tfrac{1}{2}U_+^2. \tag{2.49}$$

Now, to take advantage of the fact that (2.27) gives the behaviour of $U(x)$ near 0, we will consider this last equation as $x \to 0^-$, but first we need the following expression, taken from Abramowitz & Stegun (1972), for the magnitude of the parabolic cylinder functions at $x = 0$:

$$D_{\mathrm{i}\sigma}(0) = \frac{1}{\sqrt{\pi}}\cosh\left(\frac{\pi\sigma}{2}\right)\frac{\Gamma\left(\frac{1}{2} + \frac{1}{2}\sigma\right)}{2^{-\mathrm{i}\sigma/2}},$$

which, on using $|\Gamma(\frac{1}{2} + \mathrm{i}z)|^2 = \pi\mathrm{sech}\pi z$, yields

$$|D_{\mathrm{i}\sigma}(0)|^2 = \cosh^2\left(\frac{\pi\sigma}{2}\right)\mathrm{sech}\left(\frac{\pi\sigma}{2}\right) = \cosh\left(\frac{\pi\sigma}{2}\right).$$

The resulting equation is

$$\frac{u_0^2}{8\nu\omega\sinh\left(\frac{1}{2}\pi\sigma\right)}U_-^2 = -\beta\nu + \tfrac{1}{2}U_+^2, \tag{2.50}$$

which is a nonlinear eigenvalue problem for β. It is more convenient, though, to write this equation in terms of $\sigma = \omega/\beta$, where both ω and σ are known, as well as u_0, $U_\pm$ and ν:

$$\left(\frac{u_0^2}{\nu\omega}\right)\left(\frac{U_-^2}{\nu\omega}\right)\frac{1}{8\sinh\left(\frac{1}{2}\pi\sigma\right) + 1/\sigma} = \frac{U_+^2}{2\nu\omega}. \tag{2.51}$$

Furthermore, by defining $q_0 = u_0^2/2\nu\omega$ and $Q_\pm = U_\pm^2/2\nu\omega$, with these variables related by $Q_+ = q_0 + Q_-$ (see equation (2.26)), we may write

$$1 + \left(\frac{\frac{1}{2}\pi\sigma}{\sinh\left(\frac{1}{2}\pi\sigma\right)}\right)\frac{q_0 Q_-}{\pi} = Q_+\sigma. \tag{2.52}$$

For simplicity in what follows, let $\psi = (\pi\sigma/2)/(\sinh(\pi\sigma/2))$. It is easily verified that as $\sigma \to 0$, $\psi(\sigma) \to 1$ and as $\sigma \to \infty$, $\psi(\sigma) \to 0$; moreover, $\psi(\sigma)$ decreases monotonically. In figure 2 we plot the straight line $Q_+\sigma$ and the curve $1 + (q_0 Q_-/\pi)\psi(\sigma)$; it is quite easy to see that for all real and positive $Q_\pm$, q_0 there is a unique positive root of the equation (2.52) for σ. It follows that to each $\omega > 0$ there corresponds a unique positive value of the gradient parameter β.

Three different limiting cases will arise, which can be best understood by means of figure 2, where $\psi(\sigma)$ has been approximated by $\psi(\sigma) \sim 1$ for $\sigma \leqslant 1$, $\psi(\sigma) \sim 0$ for $\sigma > 1$. Then, we see that if $Q_+ < 1 + q_0 Q_-/\pi$ the solution of (2.52) is $\sigma Q_+ \sim 1$ and thus $\sigma \sim Q_+^{-1}$, while if $Q_+ \geqslant 1 + q_0 Q_-/\pi$ the solution is $\sigma \sim (1 + q_0 Q_-/\pi)Q_+^{-1}$. The three relevant ranges which arise are

$$\text{A: } q_0 Q_- \ll 1 \Rightarrow \sigma \sim Q_+^{-1}, \tag{2.53}$$

$$\text{B: } 1 \ll q_0 Q_- \ll Q_+ \Rightarrow \sigma \sim (1 + q_0 Q_-/\pi)Q_+^{-1}, \tag{2.54}$$

$$\text{C: } q_0 Q_- \gg Q_+ \Rightarrow \sigma \sim Q_+^{-1}. \tag{2.55}$$

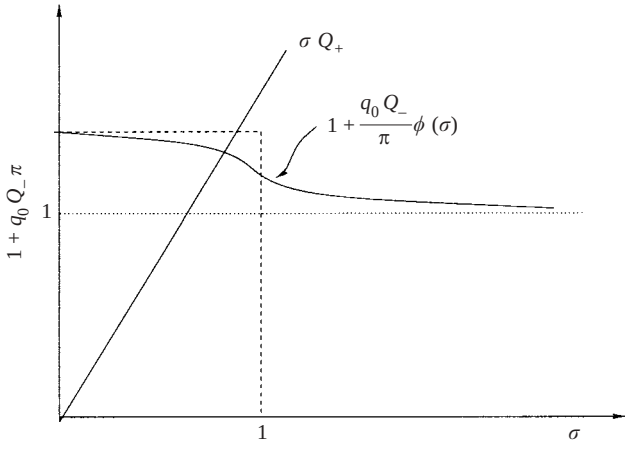

FIGURE 2. Graphical solution of the nonlinear eigenvalue problem for β. Both $\psi(\sigma)$ and its approximation by a step function are shown; the approximation is shown as a dotted line.

At this point we introduce a new parameter $\alpha > 0$, defined by the following relation:

$$Q_- \sim \epsilon^{-\alpha}. \tag{2.56}$$

Recall that $\epsilon = u_0/U_- \ll 1$ (note that $\epsilon^2 = q_0/Q_-$, and that this is essentially the amplitude of the fluctuations), and $R_- = U_-^2/2\nu\omega = Q_-$; thus, α is related to both the amplitude and the frequency of the fluctuations. It is now possible to find a set of values of α that correspond to the different regions described above. In region A, by writing the condition (2.53) in terms of the new parameters ϵ and α, we arrive at $\epsilon^{2(1-\alpha)} \ll 1$, and thus, since $\epsilon \ll 1$, we conclude that $\alpha < 1$. In the same manner, for region C we obtain $\epsilon^{\alpha-2} \ll 1$, and therefore $\alpha > 2$. It follows immediately that range C corresponds to $1 < \alpha < 2$.

It is important to point out that although the three ranges defined above in terms of values of q_0 and $Q_\pm$ determine three different ranges of α, the contrary is not generally true. This consideration will be especially important later on, in the context of numerical experiments, where we will study the different behaviours of solutions depending on the range within which they fall.

For ranges A and C, $\beta \sim \omega Q_+ = U_+^2/2\nu$ which is precisely the same value as would be expected for a Taylor shock solution in the absence of fluctuations. In this case we do not observe any significant broadening of the shock profile on account of the fluctuations introduced behind the shock. Using the same method as in § 2.1 it is seen that the shock remains thin, that the deviations are $O(\epsilon^2)$ everywhere, and that the shock is controlled by molecular diffusion and not the wave fluctuations. We are looking for values of the parameters ϵ and R_- (or, equivalently, u_0 and ω) such that the eigenvalue β has a value much less than the predicted Taylor value. This sort of effect clearly will take place only for parameters in range B, where $\sigma \sim q_0/\pi$ is the approximate root of (2.52), and thus $\beta \sim \omega\pi/q_0$. Since the region defined by (2.54) can also be written as $Q_-^{-1} \ll q_0 \ll 1$, it is clear that $\sigma \ll 1$, but also that σ in this case will be much larger than the value Q_+^{-1} which it takes in the regions where there is no significant shock broadening. Also, the gradient factor β is smaller by a factor $O(1/q_0 Q_-) \ll 1$ than its value in the unperturbed Taylor shock.

2.5. *The mean profile for parameters in region B*

In this section we will assume that u_0 and ω fall within region B, in which we expect to observe the desired effects of shock broadening and mean profile distortion. In this case, recall from the previous section that $\sigma \sim q_0/\pi \ll 1$ and that $\beta \sim \pi\omega/q_0$. Writing the mean profile equation (2.49) in terms of the previously defined variables, q_0 and $Q_\pm$, we obtain

$$\tfrac{1}{2}U^2(x) + \frac{Q_- q_0 \nu\omega}{\sinh \pi\sigma}\left(\frac{\beta|x|}{U(x)}\right)^2 |D_{i\sigma}(\xi)|^2 e^{-\xi^2/2} = \nu\frac{dU}{dx} + \tfrac{1}{2}U_+^2. \tag{2.57}$$

For σ very small, we can write $\sinh \pi\sigma \sim \pi\sigma \sim q_0$, and so the previous equation now reads

$$\tfrac{1}{2}U^2(x) + \pi^2 Q_- \nu\omega\left(\frac{\omega|x|}{q_0 U(x)}\right)^2 |D_{i\sigma}(\xi)|^2 e^{-\xi^2/4} = \nu\frac{dU}{dx} + \frac{1}{2}U_+^2. \tag{2.58}$$

We now introduce two new variables,

$$y = \frac{U(x)}{U_+}, \qquad X = \frac{U_+ x}{2\nu}; \tag{2.59}$$

the second, X, is known as the Taylor variable. We now write the mean profile equation (2.58) as

$$\frac{\pi\xi^2}{2}\left(\frac{Q_-}{q_0 Q_+^2}\right)|D_{i\sigma}(\xi)|^2 e^{-\xi^2/4} = y^2\left[\frac{dy}{dX} + 1 - y^2\right]. \tag{2.60}$$

In order to establish natural inner and outer coordinates for this problem we observe that in region B, $\beta \sim \omega\pi/q_0$, so that

$$X = \frac{U_+}{2\nu}\sqrt{\frac{\nu q_0}{\omega\pi}}\,\xi.$$

Making use of the fact that in this region $\sqrt{q_0} = \epsilon\sqrt{Q_-}$ and $Q_\pm \sim \epsilon^{-\alpha}$ we find

$$X = \sqrt{\frac{U_+^2}{2\nu\omega}\frac{Q_-}{2\pi}}\,\epsilon\,\xi = \sqrt{\frac{Q_+ Q_-}{2\pi}}\,\epsilon\,\xi \sim \frac{\epsilon^{1-\alpha}}{\sqrt{2\pi}}\,\xi. \tag{2.61}$$

Since $1-\alpha < 0$ it becomes clear that X is the natural inner coordinate for the mean profile and ξ is an outer coordinate. Later on we will see that a further inner-inner coordinate will be needed to resolve the structure of the mean profile near $X = 0$. In the meantime, for this region we have

$$\sigma \sim \frac{q_0}{\pi} = \frac{\epsilon^2 Q_-}{\pi} \sim \frac{\epsilon^{2-\alpha}}{\pi},$$

so that $\sigma = O(\epsilon^{2-\alpha}) \to 0$, and then, using (2.36), for $\xi = O(1)$ and $\sigma \ll 1$ we write

$$D_{i\sigma}(\xi) \sim e^{-\xi^2/4} + O(\sigma). \tag{2.62}$$

Thus, for $\xi = O(1)$,

$$\frac{\pi\xi^2}{2}\left(\frac{Q_-}{q_0 Q_+^2}\right)e^{-\xi^2/2} = y^2\left[\frac{dy}{dX} + 1 - y^2\right], \tag{2.63}$$

but $(Q_-/q_0 Q_+^2) \sim \epsilon^{2(\alpha-1)}$, so we write

$$\frac{\pi Q_-}{2q_0 Q_+^2} = \lambda\epsilon^{2(\alpha-1)}.$$

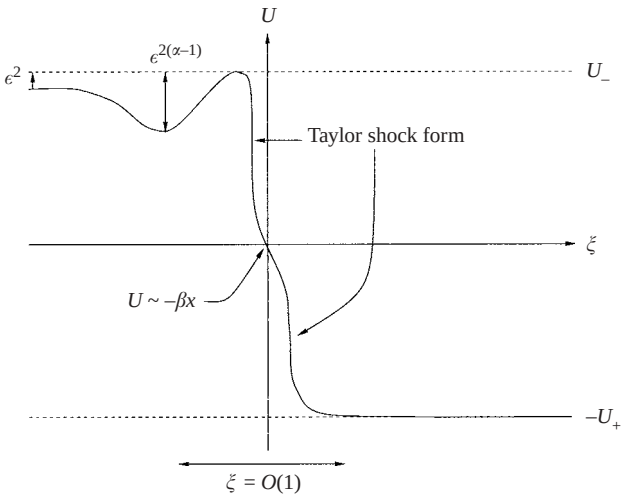

FIGURE 3. Overall portrait of mean profile structure for values of the parameters in region B. Large-scale deviation effects can be observed at $\xi = 0$, and smaller-scale ones are predicted at $\xi = -1$. The initial amplitude of the perturbations is $O(\epsilon^2)$.

It is also possible, on account of (2.61), to write $X = \mu\epsilon^{1-\alpha}\xi$. We can now rewrite equation (2.63) as

$$\lambda\epsilon^{2(\alpha-1)}\xi^2 e^{-\xi^2/2} = \frac{\epsilon^{\alpha-1}}{\mu} y^2 \frac{dy}{d\xi} + y^2(1-y^2). \tag{2.64}$$

We now look for an asymptotic approximation to the solution of equation (2.64), in the form

$$y(\xi) \sim y_0(\xi) + \epsilon^{\alpha-1} y_1(\xi) + \epsilon^{2(\alpha-1)} y_2(\xi) + \cdots.$$

After substituting in equation (2.64) and equating powers of ϵ, we arrive at the outer solution

$$y(\xi) = 1 - \epsilon^{2(\alpha-1)} \tfrac{1}{2}\lambda\xi^2 e^{-\xi^2} + o\left(\epsilon^{2(\alpha-1)}\right), \tag{2.65}$$

where we can see that the mean profile distortion for $\xi = O(1)$ is of the order of $\epsilon^{2(\alpha-1)}$, which can be quite large since α can be arbitrarily close to 1, whereas for $\xi \to -\infty$ we have

$$\lim_{\xi\to-\infty} y(\xi) = \frac{U_-}{U_+} = \left(\frac{Q_-}{Q_+}\right)^{1/2} = 1 - \tfrac{1}{2}\epsilon^2 + \cdots. \tag{2.66}$$

Therefore, the mean profile distortion increases considerably from the value of ϵ^2 it has as $\xi \to -\infty$, to $\epsilon^{2(\alpha-1)}$ for $\xi = O(1)$, as is illustrated in figure 3. The small-scale effects observed in § 2.1 have been amplified here due to the broadening of the region behind the shock where the gradient is affected by the fluctuation energy. To complete the portrait of y in this region we look at its derivative as obtained from (2.65),

$$\frac{dy}{d\xi} \sim \lambda e^{2(\alpha-1)-\xi^2}\xi(1-\xi^2) + o\left(\epsilon^{2(\alpha-1)}\right), \tag{2.67}$$

so that

$$\frac{dy(0)}{d\xi} = \frac{dy(-1)}{d\xi} = 0.$$

From the above we conclude that y decreases with increasing ξ from the value given by (2.66) for ξ large and negative up to the point $\xi = -1$, where it attains a minimum value $y_{min} = 1 - \frac{1}{2}\lambda e^{-1}\epsilon^{2(\alpha-1)} + o(\epsilon^{2(\alpha-1)})$. Between $\xi = -1$ and $\xi = 0$, y increases, approaching a maximum value $y_{max} = 1 + o(\epsilon^{2(\alpha-1)})$ as $\xi \to 0^-$. Notice then that the value of y at $\xi = 0$ represents an overshoot from the value of y as $\xi \to -\infty$, and that the minimum at $\xi = -1$ may be quite pronounced if α is close to 1.

As we have already mentioned, the region $X = O(1)$ deserves special study; in this region, in general, we have $y = O(1)$, so that we may write $y(X) = \hat{y}(X) + o(1)$, and substituting in equation (2.64) leads to

$$\hat{y}^2\left(\frac{\mathrm{d}\hat{y}}{\mathrm{d}X} + 1 - \hat{y}^2\right) = 0,$$

which has a singular point at $X = 0$. Considering, for the moment, $\hat{y} > 0$ only, we have

$$\frac{\mathrm{d}\hat{y}}{\mathrm{d}X} + 1 - \hat{y}^2 = 0. \tag{2.68}$$

The solution to this equation must match, as $X \to -\infty$, with the value taken by the outer solution as $\xi \to 0^-$. From (2.65) we see that this value is 1, and thus the solution to (2.68) we are looking for is

$$\hat{y}(X) = -\tanh(X - X_0), \tag{2.69}$$

since $\hat{y}(X) \to 1$ as $X \to -\infty$. X_0 is a constant undetermined by the matching, but we can easily eliminate it by setting $\hat{y}(0) = 0$. Now, however, a difficulty arises: the value of $(\mathrm{d}y/\mathrm{d}X)(0)$ calculated using the Taylor solution (2.69) is -1, while the nonlinear eigenvalue problem yields the much smaller value $(\sqrt{\lambda}\epsilon^{2(\alpha-1)})/\mu$. A curious feature of this problem, as is now seen, is that it will be necessary to give the inner solution further internal substructure to resolve the discontinuity at $\xi = 0$ and construct a solution with the necessary gradient adjustment at the origin.

We return to the complete equation (2.64), which we now write in terms of X instead of ξ, and using $\varepsilon = \epsilon^{\alpha-1}$:

$$\lambda\left(\frac{\varepsilon^2 X}{\mu}\right)^2 \exp(-(\varepsilon X/\mu)^2) = y^2\left(\frac{\mathrm{d}y}{\mathrm{d}X} + 1 - y^2\right). \tag{2.70}$$

For y, X both very small it is possible to make a uniform approximation of this equation,

$$y^2\frac{\mathrm{d}y}{\mathrm{d}X} + y^2 = \delta^2 X^2, \tag{2.71}$$

with $\delta = \sqrt{\lambda}\varepsilon^2/\mu \ll 1$. This equation can, in principle, be solved exactly by writing the solution in the form $y = XY(X, \delta)$, and substituting in the above equation:

$$Y^2\left(X\frac{\mathrm{d}Y}{\mathrm{d}X} + Y + 1\right) = \delta^2,$$

or

$$\frac{Y^2\mathrm{d}Y}{P(Y)} = -\frac{\mathrm{d}X}{X}, \tag{2.72}$$

where $P(Y) = Y^3 + Y^2 - \delta^2$. However, the presence of δ^2 in $P(Y)$ makes it impossible to integrate by partial fractions, so we resort instead to a perturbation approach to the original equation (2.71). In the discussion that follows we refer to the first term on

the left as (I), the second term on the left as (II), and to the term on the right-hand side as (III). Assuming $X = O(\delta^{\beta})$ and $y = O(\delta^{\gamma})$, with $\beta, \gamma > 0$ we find that it is possible to balance (II) with (III) in such a way that (I) is smaller than (II) by a factor of δ, with $\delta \ll 1$, in which case we then have $y \sim \pm\delta X$. Since we want to match this solution to (2.71) with the Taylor solution (2.69) at some point in the interior of the shock, and since in this region $\hat{y} = -X + O(X^3)$, we consider $X = O(y)$. Then we can balance (I) with (II), and term (III) is smaller than either by a factor δ^2; if we ask for y not identically zero, this yields the solution $y \sim -X$.

This solution will then behave like $-X$ for $X = O(y)$ and X negative, and like $-\delta X$ for X very small and negative. Notice that this solution will then match the limit of the Taylor solution (2.69) to the left, and will behave in the required manner ($U \sim -\beta x$) as $X \to 0^-$. Thus, we are presented not only with a broadening of the shock region, but with a very particular deformation of it, where as $X \to 0^-$ we observe initially a steepening that coincides with that which would be expected of a Taylor shock, but which becomes much less pronounced as the solution passes through $X = 0$, and then becomes steeper once again before matching onto the outer solution for $X > 0$ (the matching against the inner asymptotics of (2.69) is done in a completely analogous manner to that already done for $X < 0$). The outer limit of solution (2.69) as $X \to \infty$ is $y = -1$ (or $U = -U_+$), with exponentially small error. It is seen that the fluctuations, which almost vanished for $\xi \to 0^-$, where the mean profile attained its maximum value, dominate once more in the middle of the shock region, but fail to penetrate $X = 0$ to any algebraic order.

A complete portrait of the mean profile structure is now possible when the parameters are such that they allow the shock to broaden; see figure 3.

3. Numerical results

There exist a variety of ways in which to approach numerical solutions of nonlinear parabolic equations such as Burgers equations. Since the problems that we are interested in involve shocks and their evolution over arbitrarily long time periods, the numerical methods used must be able to cope with such exigencies, as well as satisfy the usual conditions for stability, convergence and small truncation error; they must also be reasonably economical with respect to computational time. The first scheme to be implemented was the well-known Douglas–Jones (1963) predictor–corrector implicit method, which is a modification of the Crank–Nicholson method. This method, however, is not found to be appropriate when very sharp discontinuities occur in the wave profile. To circumvent the difficulties posed by such a discontinuity, it is common to use what is known as a pseudospectral method. Its distinctive characteristic is the method of evaluation of spatial derivatives. The spatial derivatives are calculated with a very high degree of accuracy by means of finite Fourier transforms, and it is precisely because of this that the method is appropriate for the case of discontinuous profiles. The accuracy is controlled by the number of mesh points used for the calculation of the Fourier transform. In contrast to what are called spectral schemes, though, the nonlinear terms are not evaluated by convolution in spectral space; hence the name pseudospectral. For the details on the implementation of this method we refer the reader to the articles by Hammerton & Crighton(1989*a*, *b*), which are, in turn, based on the work of Gazdag (1973).

All our calculations involve the use of double-precision arithmetic; for stability considerations, we have simply followed the guidelines set out by Hammerton & Crighton: if we make the time step smaller, the spatial step must decrease accordingly.

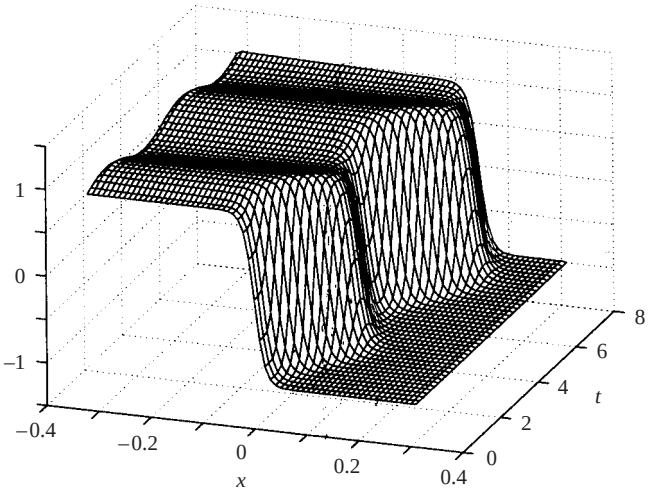

FIGURE 4. Evolution of a steady Taylor shock profile with fluctuations introduced behind the shock.

Typically, the time step will be $\Delta t = 0.001$ and the spatial step $\Delta x = 0.01$. It is important to choose a sufficiently small mesh size to be able to resolve shock details in regions where the discontinuity is sharp; thus, for early stages of evolution, a greater number of mesh points might be required (as a rule of thumb, at least ten points should be used within a thin shock region). The mesh size can be increased as the shock widens.

As we have seen in the previous section, a broadening of the shock region in the mean profile will only be observed for some particular values of the parameters ϵ and R_-; for numerical analysis of this situation, we have, without loss of generality, fixed $U_\pm = 1$ and $\nu = 1/100$. In this way, the parameters that now determine the structure of the mean profile are the characteristic fluctuation amplitude u_0 and the typical frequency ω. The necessary condition for a significant broadening of the mean shock profile to occur, (2.54), becomes

$$1 \ll 2500\left(\frac{u_0}{\omega}\right)^2 \ll \frac{50}{\omega}. \tag{3.1}$$

One set of parameters that satisfies condition (3.1) is $u_0 = 1/10$ and $\omega = \pi/2$; for this particular region, all following results correspond to this set of parameters. In figure 4 we observe the evolution of a steady Taylor shock profile affected by the introduction of small fluctuations, of amplitude u_0 and frequency ω, behind the shock. Ideally, these fluctuations would be introduced at a very large distance from the shock, but since this would make the process very expensive from a computational standpoint, we actually generate these fluctuations at $x = -0.32$, with the centre of the shock located at $x = 0$. The Taylor shock, when ν is sufficiently small, is essentially a step function apart from the thin shock region, and thus almost constant away from the centre of the shock. The position of the shock centre is defined as x_0 such that $U(x_0) = 0$, where U is again the mean profile. The fluctuations travel to the right with speed unity, until they reach the shock region and interact with it. At this point, the shock centre starts moving as well, and we will later propose the hypothesis that this movement of the shock centre, when averaged over one time period, is precisely what causes the shock broadening we observe.

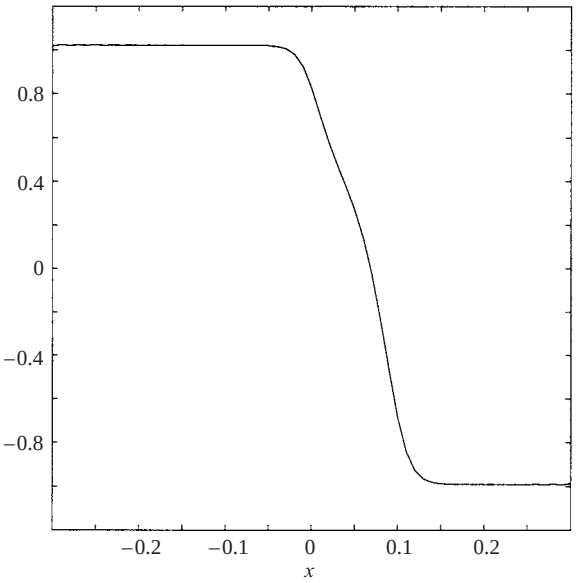

FIGURE 5. Mean profile corresponding to region B: $u_0 = 1/10$, $\omega = \pi/2$.

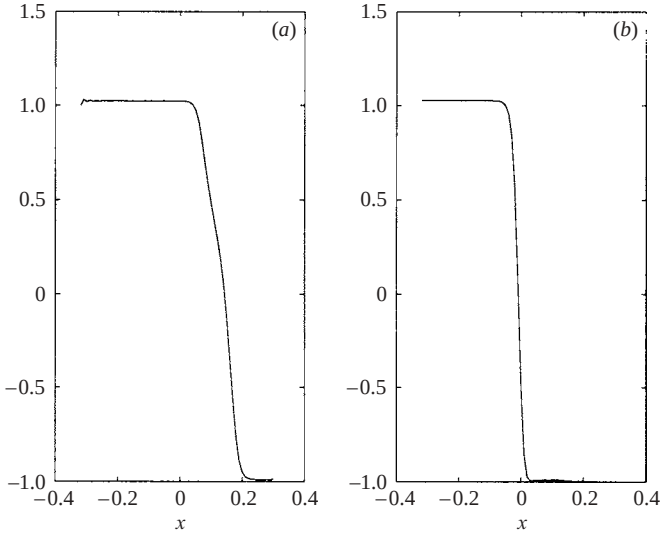

FIGURE 6. Shock profile averaged over one time cycle with (*a*) fixed axes, (*b*) axes moving with the shock centre.

When we average this profile over one time cycle (in this case we have averaged over the second cylcle, $t = 4$ to $t = 8$), we observe the expected behaviour (see figure 3) for the $\xi = O(1)$ region; that is to say, a region where the gradient becomes significantly smaller than in the Taylor shock solutions to which it is matched on either side. See figure 5.

A very interesting result, however, was obtained when the averaging was done with respect not to the fixed axes, but to axes moving with the shock centre. In this case, what we obtain is exactly a Taylor shock, with no broadening of the shock whatsoever

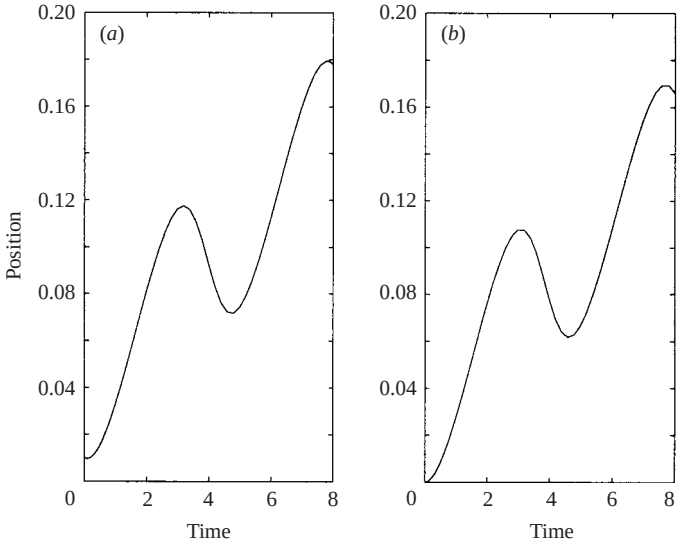

FIGURE 7. Position of the shock centre as a function of time: (*a*) actual position, (*b*) prediction.

(see figure 6*b*). This suggests that this effect is only due to the movement of the shock centre, and not to any essential structural change in the mean profile.

Thus, we could propose the following form for the mean profile:

$$\langle U\rangle = \left\langle U_+ \tanh\left[\frac{U_+}{2\nu}(x - x_0(t))\right]\right\rangle$$
$$= \frac{U_+\omega}{2\pi}\int_0^{2\pi/\omega} \tanh\left[\frac{U_+}{2\nu}(x - x_0(t))\right] \mathrm{d}t, \tag{3.2}$$

where $x_0(t)$ is the position of the shock centre, the trajectory of which, for the parameters adopted throughout this section, is portrayed in figure 7(*a*). From weak shock theory we know that in this case the speed of the shock is given by the following equation:

$$\dot{x}_0(t) = \frac{u_0}{2}\sin\omega\left(t - \frac{x_0}{u_0}\right), \tag{3.3}$$

with the initial condition

$$x_0(0) = 0. \tag{3.4}$$

This equation can be solved algebraically to give the path of the shock centre for any set of parameters. Introducing $-y(t) = t - x_0(t)/u_0$ the equation takes on the form

$$\dot{y} + 1 = -\tfrac{1}{2}\sin\omega y, \tag{3.5}$$

with

$$y(0) = 0. \tag{3.6}$$

This resulting equation is separable, so it is possible to integrate it in the following manner:

$$\frac{\mathrm{d}}{\mathrm{d}t}\left[\int \frac{\mathrm{d}y}{1 + \frac{1}{2}\sin\omega y}\right] = -\frac{\mathrm{d}y}{\mathrm{d}t}.$$

We use the standard substitution $\theta = \tan(\omega y/2)$ to integrate the left-hand side. The solution is given, in terms of $x_0(t)$, by

$$x_0(t) = \frac{2u_0}{\omega} \arctan\left[\frac{\sqrt{3}}{2} \tan\left(\frac{\sqrt{3}\omega}{4}t + \frac{\pi}{6}\right) - \frac{1}{2}\right] + u_0 t. \tag{3.7}$$

In figure 7 we plot both (*a*) the actual path followed by the shock centre in the numerical simulation, and (*b*) the analytic solution obtained above. It is clear that, although the predicted path of the shock centre's movement does not exactly match the actual trajectory, the shape of the curves and the order of the velocities involved are very similar.

The mean profile would then be described in a general manner, for all sets of parameters, by the following integral, which is given in (3.2), and into which we have incorporated the explicit form of the shock path solution:

$$\langle U \rangle = \frac{U_+\omega}{2\pi} \int_0^{2\pi/\omega} \tanh\left\{\frac{U_+}{2\nu}\left\{x - \frac{2u_0}{\omega}\arctan\left[\frac{-2\tan\left(\frac{1}{4}\sqrt{3}\,\omega t\right)}{\sqrt{3} + \tan\left(\frac{1}{4}\sqrt{3}\,\omega t\right)}\right] - u_0 t\right\}\right\} \mathrm{d}t. \tag{3.8}$$

The usefulness of this integral form of the mean profile is, however, seriously compromised by the obvious difficulty of performing the integration.

Returning to the set of parameters in region B that we have previously dealt with ($u_0 = 1/10$ and $\omega = \pi/2$), we calculate the predicted value of the corresponding gradient at the origin, β, as

$$\beta = \frac{\pi\omega}{q_0} = \frac{\pi^3}{2} \simeq 15.5,$$

but the value found from the numerical analysis is $\beta \simeq 7$, and the value of the gradient outside this region reaches almost 25, so the desired effect is, in fact, observed, since the gradient for the Taylor shock is given by $\beta_{Taylor} = U_+/2\nu = 50$. Experimenting with averaging over different time cycles yields somewhat different results (although the differences are small), so we suspect that after a long time has elapsed we might arrive at a steady state. As time passes, the shock keeps moving to the right, so that for very long times we might actually run out of space. To allow for as many cycles as possible to be averaged within a given x interval (in this case, $x \in [-2.56, 2.55]$) we take $u_0 = 1/20$, so that the shock moves less rapidly. It then also becomes necessary to adjust the value of ω, which we take to be $\pi/4$ in order that condition (3.1) be satisfied. Although looking at the average mean profiles is not very helpful, looking at their derivatives reveals that in general the steepest slope is achieved immediately after the shock region is reached; the slope then increases steadily until it reaches a maximum value, and then decreases again, although not down to the minimum level arrived at before. This would seem to confirm that the inner solution defined in § 2.2 does not match onto the outer solution in a symmetric manner to either side of the shock. In fact, although we have established that the solutions do match, the manner in which they do so has not been specified. In figure 8 we plot both the first minimum and the local maximum values for the first 16 time cycles.

We now observe that although the first local minimum value decreases with each successive cycle, reaching a value of -30, the local maximum value, which we identify with $-\beta$, stays more or less constant, at -7. In this case, for the parameters we

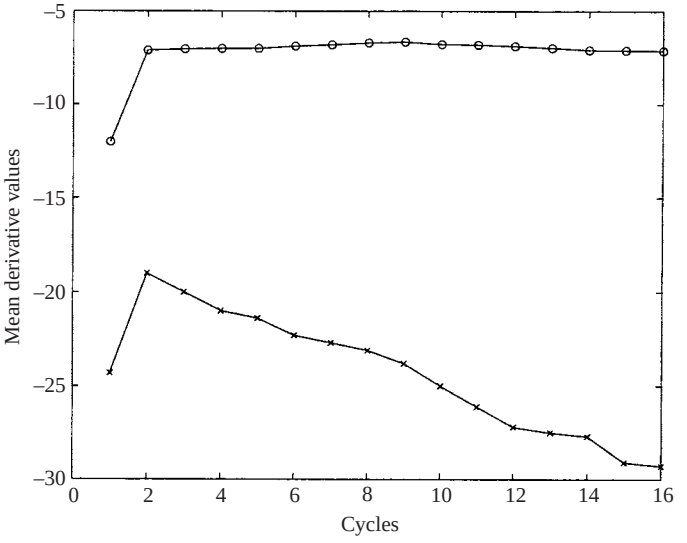

FIGURE 8. Evolution of the first local minimum (×) and maximum (○) values over the first 16 time cycles. Averaging over time period $T = 8$.

are using, the predicted value of β would be 15.5, so we must conclude that even though the order of the ratio between β and the value expected without the effect of the fluctuations is correct, and the sought behaviour is very noticeable, we are not predicting the slopes within the shock region very accurately. It has been recently suggested that some numerical diffusion might be the cause for this discrepancy.

The results of averaging when the parameters fall into regions A and C have been confirmed by running numerical tests with parameters in these ranges: we obtain undisturbed Taylor shocks, as expected.

4. Conclusions

Below we list some points which we think require further investigation, or which merit further discussion:

(*a*) Equation (3.2) is evidently quite difficult to integrate, for almost any $x_0(t)$ that would turn out to be relevant, but it still needs to be carefully analysed to perhaps explain why it is that broadening of the shock region is only observed for parameters such that (2.54) is satisfied. So far, it is only clear that very small fluctuation amplitudes with $\omega = O(1)$, as well as relatively large amplitudes with very small frequencies inhibit the type of behaviour seen above; it remains to explain why this is so.

(*b*) The small-scale deformation represented by the minimum observed at $\xi = -1$ described in § 2.5 cannot be confirmed numerically using a mesh of the size used to obtain the results in the previous sections. Consider that, according to the change of variables (2.33), with $\omega = \pi/2$ and $u_0 = 1/10$, $\xi = -1$ corresponds roughly to $x = -1/1550$; it is clear that our mesh is not sufficiently fine to adequately portray any deformation at this scale.

(*c*) Finally, we call attention to the modification of the shape of a Taylor shock caused by perturbations which contain very small amounts of energy, a fact reflected clearly in the smallness of the parameter ϵ. The Taylor shock solution is constructed

in such a way that it travels for an undetermined distance at a fixed velocity without altering its shape. We also mentioned that for such a shock the most marked changes in velocity and pressure occur in the vicinity of the shock itself. When the advected perturbations enter this region, they are capable, depending on their amplitude and characteristic frequency, of throwing off the equilibrium that keeps the shape of the shock profile constant, although the precise manner in which this is done is not known. The effect of this profile distortion is perhaps most noticeable in the shock rise time, which in this case is of the order of 4ν for the unperturbed shock and of $u_0^2 U_+/\pi\nu\omega$ for the broadened shock profile (only when the relevant parameters fall within region B, as defined in § 2.4). The mechanisms which induce this thickening have not been described, and further examination of integral (3.8) might yield interesting results in this respect.

REFERENCES

Abramowitz, M. & Stegun, I. A. 1972 *Handbook of Mathematical Functions*. Dover.

Bateman, H. 1915 Some recent researches on the motion of fluids. *Mon. Weath. Rev.* **43**, 163–170.

Burgers, J. M. 1948 A mathematical model illustrating the theory of turbulence. In *Advances in Applied Mechanics* (ed. R. von Mises & T. von Kármán), Vol. 1, pp. 171–199. Academic.

Douglas, J. & Jones, B. F. 1963 On predictor-corrector methods for nonlinear parabolic differential equations. *J. SIAM* **11**, 195–204.

Dowling, A. P. & Ffowcs Williams, J. E. 1983 *Sound and Sources of Sound*. Ellis Horwood.

Ffowcs Williams, J. E. 1992 Noise source mechanisms. In *Modern Methods in Analytical Acoustics*, pp. 313–354. Springer.

Gazdag, J. 1973 Numerical convective schemes based on accurate computation of space derivatives. *J. Comput. Phys.* **13**, 100–113.

Gurbatov, S., Malakhov, A. & Saichev, A. 1991 *Nonlinear Random Waves and Turbulence in Nondispersive Media: Waves, Rays and Particles*. Manchester University Press.

Hammerton, P. W. & Crighton, D. G. 1989*a* Old-age behaviour of cylindrical and spherical nonlinear waves. *Proc. R. Soc. Lond.* A **422**, 387–405.

Hammerton, P. W. & Crighton, D. G. 1989*b* Approximate solution methods for nonlinear acoustic propagation over long ranges. *Proc. R. Soc. Lond.* A **426**, 125–152.

Lumley, J. L. 1970 *Stochastic Tools in Turbulence*. Academic.

Martín Vide, J. P., Dolz, J. & del Estal, J. 1993 Kinematics of the moving hydraulic jump. *J. Hydraul. Res.* **31**, 171–186.

Moran, J. P. & Shen, S. F. 1966 On the formation of weak shock waves by impulsive motion of a piston. *J. Fluid Mech.* **25**, 705–718.

Taylor, G. I. 1910 The conditions necessary for discontinuous motion in gases. *Proc. R. Soci. Lond.* A **84**, 371–377.

Van Dyke, M. 1975 *Perturbation Methods in Fluid Mechanics*. The Parabolic Press.

Whitham, G. B. 1974 *Linear and Nonlinear Waves*. John Wiley & Sons.

Whittaker, E. T. & Watson, G. N. 1980 *A Course of Modern Analysis*. Cambridge University Press.